Variational Image Decomposition Model OSV with General Diffusion Regularization

Guodong Wang
College of Information Engineering, Qingdao University, Qingdao, China;
Email: doctorwgd@gmail.com

Jie Xu
College of Physics Science, Qingdao University, Qingdao, China;
Email: xujiehust@gmail.com

Zhenkuan Pan and Jinbao Yang
College of Information Engineering, Qingdao University, Qingdao, China;
Email: {allen_wgd@163.com, yang_qdu@163.com}

***Abstract*—Image decomposition technology is a very useful tool for image analysis. Images contain structural component and textural component which can be decomposed by variational methods such as VO (Vese-Osher) and OSV (Osher-Sole-Vese) models. OSV model is a powerful tool for image decomposition but the minimization is a hard problem because of solving the 4th order partial differential equations with complex finite difference scheme for Laplacian of curvature. In this paper we proposed an improved OSV model with general diffusion regularization. The general diffusion terms can be TV(Total Variation), Nonlinear diffusion(Perona and Malik) and Charbonnier regulerizers. Additionally, we also use L1 norm as data term inspired by TV-L1 method. We also use Split Bregman method for the easy implementation of the improved OSV model. Experiments show the proposed method is a valid method for image decomposition.**

***Index Terms*—image decomposition, OSV model, Split Bregman method, TV-L1, general diffusion regularization**

I. INTRODUCTION

Image decomposition technology can decompose the image into structural component, textural component, noise and other image components. The decomposed texture part is very useful in image analysis such as texture segmentation, texture discrimination and other applications.

The variational image decomposition methods are the popular ones. Total Variation (TV) model [1] is the basic nonlinear variational model of image diffusion. It laid the foundation for variational method of image processing and computer vision. Although it can separate noise from image, the texture part can't be decomposed by it. Meyer [2] established modeling the texture component as having a small norm in a suitably defined Banach space [3]. But Meyer didn't give the realization method. Le [4] proposed Besov space to describe the oscillation part of the image. Vese [5] proposed a VO model which approximates Meyer's theoretical model, that is, they proposed an L^p approximation to the norm $\|\cdot\|_G$, meanwhile, they gave the corresponding Euler-Lagrange equations. Osher [6] extended VO model, and presented a variational model for image decomposition which based on the total variation and the norm H^{-1}. The authors show that this new model is simpler than VO model, however, the decomposition model based on this function suffers from low running time because the Euler-Lagrange equation is a fourth-order nonlinear PDE, its difference format is complex. Aujol [7] proposed two norms of Sobolev and Besov norms and split the image into three components, they are structure, texture and noise parts. Chan [8] introduced high order diffusion term to reduce the staircase effect and introduced the dual variables which can rapidly implement the decomposition of the image texture and structure information of the OSV model. Ng [9] introduced a decomposition model to restore blurred images with missing pixels. They used the total variation norm and its dual norm to regularize the cartoon and texture respectively. Then they recommended an efficient numerical algorithm based on the splitting version of augmented Lagrangian method to solve the problem.

In addition, to enhance the quality of image diffusion for classical ROF model, Osher [10] extended the ROF model to an iterative regulation method based on the Bregman Distance. They added the noise after diffusion to the original image to image diffusion again and repeated this process. This algorithm improved the quality of regularized solutions in terms of texture preservation, and reduced the influence of penalty parameter in the diffusing process. Although the computational efficiency has been greatly improved, it was still complex for implementation. To simplify implementation and improve computational efficiency, Wang [11] splitted the classical TV model into an alternating iterative process by simple divergence

doi:10.4304/jsw.9.8.2105-2111

operation and shrinkage operator of soft threshold formula through the introduction of auxiliary variable. Goldstein [12] proposed Split Bregman method of ROF model by combining split algorithm [11] and Bregman iteration [10]. Zhao [12] proposed using Split Bregman method for solving OSV model. There were many other methods and applications for signal and image decomposition [17, 18, 19].

In this paper, we propose a general diffusion regularization of OSV method and using Split Bregman method by introducing auxiliary variables and Bregman iteration parameter for solving the equation. We devote to decompose an image f into two well-structured component u and oscillating patterns (both textures and noise) v.

The organization of this paper goes as follows. In Section 2, we will introduce the original OSV model briefly. Then the Split Bregman method of OSV model with general diffusion regularization is designed in Section 3. Then some numerical examples are shown in Section 4. Section 5 is concluding remarks.

II. Original OSV Model

In [2], Meyer proposed the Banach space G as:

$$G=\left\{v \middle| v=\partial_x g_1(x,y)+\partial_y g_2(x,y),\quad g_1,g_2\in L^\infty(\Omega)\right\} \tag{1}$$

The norm is:

$$\|v\|_* = \inf_{g=(g_1,g_2)}\left\{\left\|\sqrt{g_1^2+g_2^2}\right\|_{L^\infty} \middle| v=\partial_x g_1+\partial_y g_2\right\} \tag{2}$$

Here, Ω is an open and bounded domain. Given an image f defined on Ω, Meyer's decomposition model becomes:

$$\min_u\left\{E(u)=\int_\Omega|\nabla u|+\lambda\|v\|_*,\ f=u+v\right\} \tag{3}$$

In the model, u is structural component or smooth part of the image, v is oscillating component containing texture and noise information. But in practice, model (3) is difficult for implementation. Vese [6] overcomed this difficulty by proposing an L^p approximation to the norm $\|\ \|_*$:

$$\min_{u,g_1,g_2}\left\{\begin{aligned}G_p(u,g_1,g_2)=\int_\Omega|\nabla u|\,dxdy+\lambda\int_\Omega\left|f-u-\nabla\cdot\vec{g}\right|^2 dxdy\\ +\mu\left[\int_\Omega\left(\sqrt{g_1^2+g_2^2}\right)^p dxdy\right]^{\frac{1}{p}}\end{aligned}\right\} \tag{4}$$

where, $\vec{g}=(g_1,g_2)$, $|\vec{g}|=\sqrt{g_1^2+g_2^2}$, $v(x,y)=\partial_x g_1(x,y)+\partial_y g_2(x,y),\quad g_1,g_2\in L^\infty(R^2)$. By experiments, the authors use the value $p=1$, and they show there are no obvious difference for different values of p, with $1\le p\le 10$. Osher [7] used L^p approximation to the norm $\left\|\sqrt{g_1^2+g_2^2}\right\|_{L^\infty}$ and chose $p=2$ which corresponds to the space $H^1(\Omega)$. Then he proposed the famous image decomposition model called OSV model based on the negative norm H^{-1} follows:

$$\min_u\left\{E(u)=\int_\Omega|\nabla u|dxdy+\frac{1}{2\lambda}\int_\Omega\left|\nabla\left(\Delta^{-1}(f-u)\right)\right|^2 dxdy\right\} \tag{5}$$

Equation (5) is complex because of the fourth order term of partial differential equations and low efficiency of computation.

Aujol [8] used the dual variable p, and defined the dual form of the TV norm in the following:

$$\int_\Omega|\nabla u|\,dxdy=\max_{p,|p|\le1}\int_\Omega u\ div(p)dxdy \tag{6}$$

Hence, OSV model can be transformed as:

$$\min_u\max_{p,|p|\le1}\left\{\begin{aligned}E(u,p)=\int_\Omega u\ div(p)dxdy\\ +\frac{1}{2\lambda}\int_\Omega\left|\nabla(\Delta^{-1})(u-f)\right|^2 dxdy\end{aligned}\right\} \tag{7}$$

where $p=(p_1,p_2)$.

This problem can be solved by the method in [8]. Thus, the final iterative method is:

$$p^0=0,\ p^{k+1}=\frac{p^k-\tau\left(\dfrac{\nabla f_{i,j}}{\lambda}+\nabla(\Delta div(\rho)_{i,j})\right)}{1+\tau\left|\dfrac{\nabla f_{i,j}}{\lambda}+\nabla(\Delta div(\rho)_{i,j})\right|} \tag{8}$$

$$u^{k+1}=f+\lambda\Delta div p^{k+1} \tag{9}$$

The convergence condition for (8) is proved in [9].

III. OSV Model with General Diffusion Regularization and Split Bregman Algorithm

The OSV model using total variation as diffusion term. There are many other diffusion term such as PM [14] diffusion term and Charbonnier term [15], they also give good metric in edge preserving and noise removing. So we proposed a general diffusion term for OSV model. Additional, the famous ROF model has some drawbacks such as staircase effects, loss of geometric characteristics, and so on. Chan [16] proposed TV-L1 model by changed the data term from L2 norm to L1 norm as $\int_{\Omega}|u-f|dxdy$. This model can be effectively reduce the loss of contrast and geometric feature, but its calculations are more complex than the traditional TV model. In this paper, we also use TV-L1 term as data term for our general OSV model. Thus, the proposed decomposition model becomes:

$$\min_u\left\{E(u)=\int_\Omega\varphi(|\nabla u|)dxdy+\frac{1}{\lambda}\int_\Omega\left|\nabla\left(\Delta^{-1}(f-u)\right)\right|dxdy\right\} \quad (10)$$

The diffusion term of $\varphi(|\nabla u|)$ has several patterns.

When diffusion term is TV norm, then

$$\varphi(|\nabla u|)=|\nabla u| \quad (11)$$

When diffusion term is PM norm, then

$$\varphi(|\nabla u|)=\mu^2 Log\left(1+\frac{|\nabla u|^2}{\mu^2}\right) \quad (12)$$

When diffusion term is Charbonnier, then

$$\varphi(|\nabla u|)=2\mu^2\left(\sqrt{1+\frac{|\nabla u|^2}{\mu^2}}-1\right) \quad (13)$$

We use Split Bregman method for solving equation (10). With alternating optimization method, we introduce the auxiliary variables $w_1=(w_{11},w_{12})^T, w_2, w_3=(w_{31},w_{32})^T$ and Bregman iteration parameters $b=(b_1,b_2)^T$, when the following energy functional gets its minimization, $w_1\approx\nabla u$, $w_2\approx(\Delta^{-1})(u-f)\Rightarrow\Delta w_2=u-f$, $w_3\approx\nabla w_2$. Then equation (10) became the following form

$$\min_{u,w_1,w_2,w_3}\left\{\begin{array}{l}E(u,w_1,w_2,w_3)=\int_\Omega\varphi(|w_1|)dxdy+\frac{1}{\lambda}\int_\Omega|w_3|dxdy+\frac{1}{2\theta_1}\int_\Omega\left(w_1-\nabla u-b^{k+1}\right)^2dxdy\\ \qquad +\frac{1}{2\theta_2}\int_\Omega(u-f-\Delta w_2)^2dxdy+\frac{1}{2\theta_3}\int_\Omega(w_3-\nabla w_2)^2dxdy\end{array}\right\} \quad (14)$$

where

$$b^{k+1}=b^k+\nabla u^k-w^k \quad (15)$$

One way of minimizing (14) amounts to solving the following minimization problems:

w_1, w_2 and w_3 being fixed, we search for u as solution of:

$$\min_u\left\{E_1(u)=\frac{1}{2\theta_1}\int_\Omega\left(w_1-\nabla u-b^{k+1}\right)^2dxdy+\frac{1}{2\theta_2}\int_\Omega(u-f-\Delta w_2)^2dxdy\right\} \quad (16)$$

u, w_2 and w_3 being fixed, we search for w_1 as solution of:

$$\min_{w_1}\left\{E_2(w_1)=\int_\Omega\varphi(|w_1|)dxdy+\frac{1}{2\theta_1}\int_\Omega\left(w_1-\nabla u-b^{k+1}\right)^2dxdy\right\} \quad (17)$$

u, w_1 and w_3 being fixed, we search for w_2 as solution of:

$$\min_{w_2}\left\{E_3(w_2)=\frac{1}{2\theta_2}\int_\Omega(u-f-\Delta w_2)^2dxdy+\frac{1}{2\theta_3}\int_\Omega(w_3-\nabla w_2)^2dxdy\right\} \quad (18)$$

u, w_1 and w_2 being fixed, we search for w_3 as solution of:

$$\min_{w_3}\left\{E_4(w_3)=\frac{1}{\lambda}|w_3|dxdy+\frac{1}{2\theta_3}\int_\Omega(w_3-\nabla w_2)^2dxdy\right\} \quad (19)$$

With variational method, the corresponding Euler-Lagrange equations respectively are:

$$u^{k+1}=f+\Delta w_2^k+\frac{\theta_2}{\theta_1}\left(\Delta u^k+\nabla\cdot b^{k+1}-\nabla\cdot w_1^k\right) \quad (20)$$

$$w_1^{k+1}=\nabla u^{k+1}+b^{k+1}-\theta_1\frac{\varphi'(|w_1|)w_1^{k+1}}{|w_1^{k+1}|} \quad (21)$$

$$\Delta(\Delta w_2)-\frac{\theta_2}{\theta_3}\Delta w_2=\Delta u^{k+1}-\Delta f-\frac{\theta_2}{\theta_3}\nabla\cdot w_3^k \quad (22)$$

$$w_3^{k+1}=\nabla w_2^{k+1}-\frac{\theta_3}{\lambda}\frac{w_3^{k+1}}{|w_3^{k+1}|} \quad (23)$$

For TV term, equation (21) becomes:

$$w_1^{k+1}=\nabla u^{k+1}+b^{k+1}-\theta_1\frac{w_1^{k+1}}{|w_1^{k+1}|} \quad (24)$$

For PM term, equation (21) becomes:

$$w_1^{k+1}=\nabla u^{k+1}+b^{k+1}-\theta_1\frac{2|w_1^k|}{(1+\frac{|w_1^k|}{\mu^2})}\frac{w_1^{k+1}}{|w_1^{k+1}|} \quad (25)$$

For Charbonnier term, equation (21) becomes:

$$w_1^{k+1}=\nabla u^{k+1}+b^{k+1}-\theta_1\frac{2|w_1^k|}{\sqrt{1+\frac{|w_1^k|^2}{\mu^2}}}\frac{w_1^{k+1}}{|w_1^{k+1}|} \quad (26)$$

In this paper, (20) uses the form of explicit iterative, (22) uses the form of semi-implicit iterative, (23) and (25) use a generalized shrinkage formula:

$$w_1^{k+1}=Max(|\nabla u^{k+1}+b^{k+1}|-\theta_1\varphi'(w_1),0)\frac{\nabla u^{k+1}+b^{k+1}}{|\nabla u^{k+1}+b^{k+1}|} \quad (27)$$

For different diffusion terms, we replace the corresponding terms.

For TV term, equation (27) becomes:

$$w_1^{k+1} = Max(\left|\nabla u^{k+1} + b^{k+1}\right| - \theta_1, 0)\frac{\nabla u^{k+1} + b^{k+1}}{\left|\nabla u^{k+1} + b^{k+1}\right|} \tag{28}$$

For PM term, equation (27) becomes:

$$w_1^{k+1} = Max(\left|\nabla u^{k+1} + b^{k+1}\right| - \theta_1 \frac{2\left|w_1^k\right|}{(1+\frac{\left|w_1^k\right|}{\mu^2})}, 0)\frac{\nabla u^{k+1} + b^{k+1}}{\left|\nabla u^{k+1} + b^{k+1}\right|} \tag{29}$$

For Charbonnier term, equation (27) becomes:

$$w_1^{k+1} = Max(\left|\nabla u^{k+1} + b^{k+1}\right| - \theta_1 \frac{2\left|w_1^k\right|}{\sqrt{1+\frac{\left|w_1^k\right|^2}{\mu^2}}}, 0)\frac{\nabla u^{k+1} + b^{k+1}}{\left|\nabla u^{k+1} + b^{k+1}\right|} \tag{30}$$

$$w_3^{k+1} = Max\left(\nabla w_2^{k+1} - \frac{\theta_3}{\lambda}, 0\right)\frac{\nabla w_2^{k+1}}{\left|\nabla w_2^{k+1}\right|} \tag{31}$$

The following describes the algorithm:

(1) Initialization: $u^0 = f$,

$w_{11}^0 = w_{12}^0 = w_2^0 = w_{31}^0 = w_{32}^0 = b_1^0 = b_2^0 = 0$;

(2) Iterations:

$$b^{k+1} = b^k + \nabla u^k - w^k$$

$$u^{k+1} = f + \Delta w_2^k + \frac{\theta_2}{\theta_1}\left(\Delta u^k + \nabla \cdot b^{k+1} - \nabla \cdot w_1^k\right)$$

$$\Delta\left(\Delta w_2\right) - \frac{\theta_2}{\theta_3}\Delta w_2 = \Delta u^{k+1} - \Delta f - \frac{\theta_2}{\theta_3}\nabla \cdot w_3^k$$

$$w_1^{k+1} = Max(\left|\nabla u^{k+1} + b^{k+1}\right| - \theta_1 \varphi'(w_1), 0)\frac{\nabla u^{k+1} + b^{k+1}}{\left|\nabla u^{k+1} + b^{k+1}\right|}$$

$$w_3^{k+1} = Max\left(\nabla w_2^{k+1} - \frac{\theta_3}{\lambda}, 0\right)\frac{\nabla w_2^{k+1}}{\left|\nabla w_2^{k+1}\right|}$$

(3) Stopping criterion: we stop if

$\max(\left|u^{k+1} - u^k\right|) \le \varepsilon$

IV. NUMERICAL EXPERIMENTS

All results of experiments in this paper are implemented on PC (Intel(R) Core 2 Duo, CPU E7400 2.80GHz, Memory 2.00GB) using matlab 7.0. To verify the effect of the proposed model, we test our method on three gray images shown in Fig.1. The first is a gray image which is a combination of four different Brodatz textures, the second a famous image called 'Babala' and the third is the famous image “Lena” corrupted by a Gauss noise ($\sigma = 15$).

(a) (b) (c)

Figure 1: Three original images for image decomposition: (a) Brodatz textures image. (b) Clean Barbara gray image containing structure and texture components. (c) Noisy observed Lena image, $\sigma = 15$.

Results are shown in Fig.2, Fig.3 and Fig.4. Texture image v is obtained from $f - u$ (the gray value of v is too small to display clearly, so the corresponding figure shows the decomposed texture added by 150). The choice of λ controls the texture components: the bigger the parameter λ is, the less the texture contained in u ; the smaller the parameter λ is, the less the texture contained in v . In the experiments, we set $\lambda = 0.2$.

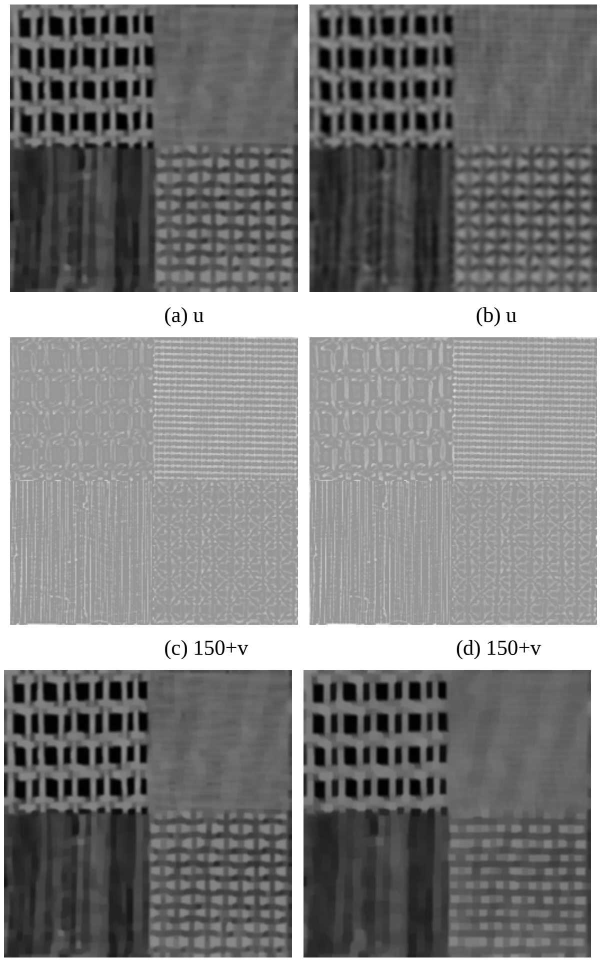

(a) u (b) u

(c) 150+v (d) 150+v

(e) u (f) u

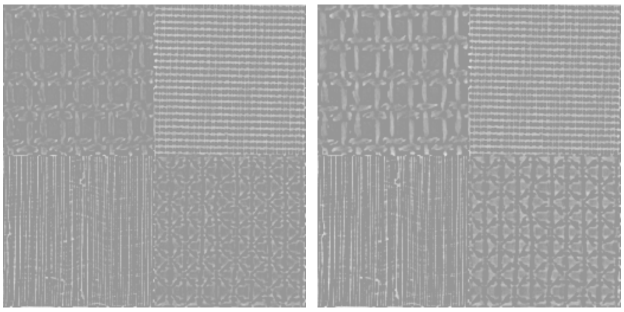

(g) 150+v (h) 150+v

Figure 2: The structural part u and texture part v using the orignal OSV model(a,c), OSV model with TVL1 norm(b,d), the OSV model with PM method(e,g), and the OSV model with Charbonnier (f,h).

From Fig.2, we can see the original OSV model has less decomposition ability than our proposed methods. The texture information in Fig. 2 (d), Fig.2 (g) and Fig.2 (h) are more clarity than that in Fig.2 (c).

(a) u (b) u

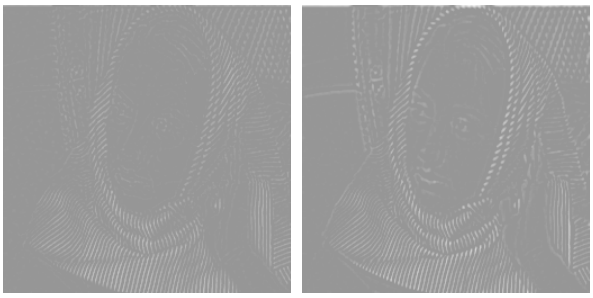

(c) 150+v (d) 150+v

(e) u (f) u

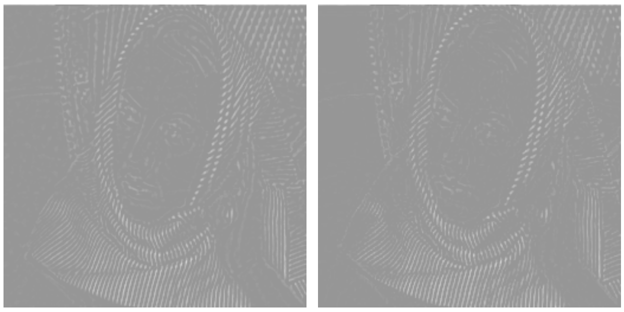

(g) 150+v (h) 150+v

Figure 3: The structural part u and texture part v using the orignal OSV model(a,c), OSV model with TVL1 norm(b,d), the OSV model with PM method(e,g), and the OSV model with Charbonnier (f,h).

At the edge of the turban and scarf at the bottom of the chin in Fig.3 (a) are still remained the texture, yet, the texture in Fig.3 (b), Fig.3 (e) and Fig.3 (f) are all disappeared.

(a) u (b) u

(c) 150+v (d) 150+v

(e) u (f) u

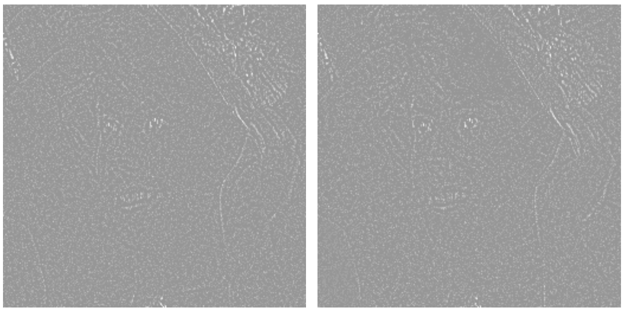

(g) 150+v (h) 150+v

Figure 4: The structural part u and texture part v using the orignal OSV model(a,c), OSV model with TVL1 norm(b,d), the OSV model with PM method(e,g), and the OSV model with Charbonnier (f,h).

In the experiments of Fig.4, the noise is also decomposed in the process of decomposing textures. The denoising effect of our proposed methods are better than the orignal OSV model. From the details of textural part, we can see our proposed models have superiority in the decomposition of the texture and other details.

From above experiments, we can see that the proposed general diffusion terms for OSV model have achieved the goal of texture decomposition. The general diffusion terms with TV norm, PM norm and Charbonnier have small difference but are all superior than the original OSV model in the ability of texture decomposition. The decomposed texture part using our methods are much more richer than the original one.

To verify the efficiency of our proposed methods, we compare the run time of each experiments. Results of time trials for the experiments mentioned above are shown in Table 1, and all the units are second(s).

TABLE I.

COMPARISON OF OPERATION TIMES OF THREE METHODS

Solving method	**CPU time of each iteration**	**Total CPU time**		
		Fig 1(a)	**Fig 1(b)**	**Fig 1(c)**
Orginal-OSV model	0.125	9.406	21.75	18.16
OSV model with TV norm	0.043	2.313	3.110	3.907
OSV model with PM norm	0.051	3.250	5.078	4.079
OSV model with Charbonnier	0.057	3.631	5.712	4.324

It can be shown from table 1, Split Bregman method of our proposed method has less time consuming than original method.

V. CONCLUSION

In this paper, we propose modified OSV models with general diffusion terms. Then the Split Bregman method is introduced to enhance the computational efficiency. Experiments show the validity and efficiency of proposed method. However, there are lots of parameters in the model and the parameter value influences the test results largely, so the next step is to establish a parameter adaptive algorithm to eliminate the influence of man-made factors on the parameter values.

ACKNOWLEDGMENT

This work was supported by National Natural Science Foundation of China (No.61305045 and No.61170106), National "Twelfth Five-Year" development plan of science and technology (No.2013BAI01B03), Qingdao science and technology development project (No. 13-1-4-190-jch).

REFERENCES

[1] Rudin L, Osher S and Fatemi E. Nonlinear Total Variation Based Noise Removal Algorithms. Physica D, 1992, vol 60, pp. 259–268.

[2] Meyer Y. Oscillating Patterns in Image Processing and Nonlinear Evolution Equations.University Lecture Scries. Boston, USA: American Mathematical Society, 2001.

[3] Koch H and Tataru D. Well-Posedness for the Navier-Stokes Equations . Adv. in Math, 2001, vol 157, pp. 22–35.

[4] Le T, Vese L. Image Decomposition Using the Total Variation and div(BMO). Journal of Multiscale Modeling and Simulation, 2005, vol 4, no 2, pp. 390–423.

[5] Vese L and Osher S. Modeling Textures with Total Variation Minimization and Oscillating Patterns in Image Processing. Journal of Scientific Computing, 2003, vol 19, no. 11, pp. 553–572.

[6] Osher S, Sole A, Vese L. Image Decomposition and Restoration Using Total Variation Minimization and the H-1 Norm. Journal of Multiscale Modeling and Simulation, 2003, vol 1, no. 3, pp. 349–370.

[7] Aujol J F and Chambolle A. Dual Norms and Image Decomposition Models. International Journal on Computer Vision, 2005, vol 63, no 1, pp. 85–104.

[8] Chan T, Esedoglu S and Park F, Image Decomposition Combining Staircase Reduction and Texture Extraction. Journal of Visual Communication and Image Representation archive, 2007, vol 18, no 6, pp. 464-486.

[9] Ng M.K, Yuan X, Zhang W. Coupled Variational Image Decomposition and Restoration Model for Blurred Cartoon-Plus-Texture Images With Missing Pixels, Image Processing, IEEE Transactions on, 2013, vol 22, no 6, pp. 2233-2246.

[10] Osher S, Burger M, Goldfarb D, Xu J and Yin W, An Iterative Regularization Method for Total Variation Based Image Restoration. Multiscale Model. Simul., 2005, vol 4, pp. 460–489.

[11] Wang Y, Yang J, Yin W and Zhang Y, A New Alternating Minimization Algorithm for Total Variation Image Reconstruction. SIAM Journal on Imaging Sciences, 2008, vol. 1, no. 3, pp. 248–272.

[12] Goldstein T, Osher S. The Split Bregman Method for L1 Regularized Problems.UCLA CAM Report 08–29, April 2008.

[13] Zhao Z, Pan Z, Wei W, Wang C. The Split Bregman Method of Variational Osv Model for Image Decomposition. Image and Signal Processing (CISP), 2010 3rd International Congress on, pp. 2870.1-7.

[14] Perona P, and Malik J. Scale-Space and Edge Detection Using Anisotropic Diffusion, IEEE Transactions on Pattern Analysis and Machine Intelligence, 12(7):629-639, July 1990.

[15] Charbonnier P, Blanc-F´eraud L, Aubert G, and Barlaud M, Two Deterministic Half-quadratic Regularization Algorithms for Computed Imaging. Proc. IEEE International Conference on Image Processing (ICIP-94, Austin, Now. 13-16, 1994), 2:168–172, 1994.

[16] Chan T, Esedoglu S, Aspects of Total Variation Regularized L^1 Function Approximation. SIAM J. Appl. Math, 2005, vol 65, no5, pp. 1817–1837.
[17] Bin Zhu, Wei-dong Jin, Radar Emitter Signal Recognition Based on EMD and Neural Network. Journal of Computers, 2012, vol. 7, no. 6, pp. 1413-1420.
[18] Hai Fang, Quan Zhou, Kaijia Li, Robust Watermarking Scheme for Multispectral Images Using Discrete Wavelet Transform and Tucker Decomposition. Journal of Computers, 2013, vol. 8, no. 11, pp. 2844-2850.
[19] Guojun Ding ,Lide Wang, Ping Shen, Peng Yang, Sensor Fault Diagnosis Based on Ensemble Empirical Mode Decomposition and Optimized Least Squares Support Vector Machine. Journal of Computers, 2013, vol. 8, no. 11, pp. 2916-2924.

Guodong Wang was born in 1980. He received his Ph.D degree in the Institute for Pattern Recognition and Artificial Intelligence, Huazhong University of Science and Technology, China in 2008. Currently he is a lecturer of the College of Information Engineering at Qingdao University. His research interests include image analysis and variational image processing.

Jie Xu was born in 1980. She received her Ph.D degree in Huazhong University of Science and Technology, China in 2009. Currently she is a lecturer of the College of Physics Science at Qingdao University. Her research interests include image analysis and variational image processing.

Zhenkuan Pan was born in 1966. He received his Ph.D. degree in engineering mechanics from Shanghai Jiao Tong University, China in 1992. Currently he is a professor of the College of Information Engineering at Qingdao University. His research interests include dynamics and control of multibody systems, computer simulation and variational image processing. He has published numerous papers and conference papers in the area of image processing and object recognition.

Jinbao Yang was born in 1979. He received his Ph.D degree in Shandong University, China in 2008. Currently he is a lecturer of the College of Information Engineering at Qingdao University. His research interests include image analysis and variational image processing.